ELSEVIER

Polymer 43 (2002) 1223–1233

polymer

www.elsevier.com/locate/polymer

Influence of chain length in nonyl-phenol ethoxylate surfactants on the film formation behaviour of methylmethacrylate-2-ethylhexyl acrylate copolymer latexes: part 1. Differential scanning calorimetry and atomic force microscopy

Lynda A. Cannon, Richard A. Pethrick*

Department of Pure and Applied Chemistry, University of Strathclyde, Thomas Graham Building, 295 Cathedral Street, Glasgow G1 1XL, UK

Received 26 June 2001; received in revised form 28 August 2001; accepted 2 November 2001

Abstract

A comparison of the film forming characteristics of methylmethacrylate-2-ethylhexyl acrylate latex copolymers stabilised with nonyl-phenol ethoxylate molecules of varying chain lengths is presented. The ability of the stabiliser to segregate and diffuse from the interfacial layer into the surrounding media influences both the rate of coalescence process and structure of the film formed. Dynamic mechanical analysis, minimum film formation temperature measurements, particle size analysis, differential scanning calorimetry (DSC) and atomic force microscopy reveal the complexity of the mechanism involved in the coalescence process. A model that describes the various stages of coalescence and compaction of the latex particles indicates the effects of chain length on the film forming properties. For the stabiliser with a chain length of 20, coalescence is observed at room temperature; whereas for the stabiliser with chain lengths of 30 and 40, coalescence only occurs if the films are raised above 315 K. For the longer chain stabilisers, the effect of stabiliser–stabiliser interaction inhibits the coalescence process and DSC data indicate the occurrence of crystalline phase structure in the thin film.

Keywords: Differential scanning calorimetry; Coalescence; Latexes

1. Introduction

In a previous paper [1], it was shown that for 2-ethylhexylacrylate/methyl methacrylate copolymers latexes, the mechanism whereby coalescence occurred depended on the glass transition temperature [T_g] of the latex. The film forming process in acrylic polymer latex materials has been extensively discussed [2–11]. In general, evaporation is the dominant rate limiting process in film formation, when the temperature of the latex is 20 K or more above its T_g. When the latex is near to T_g, the rate determining step for film formation involves deformation of the spherical particles. In acrylic polymers, there is evidence that a drying front can be formed that moves inward from the periphery and creates voids. Evaporation rates are retarded in a latex system that can undergo extensive particle deformation [12] and correlation has been observed between the film formation characteristics and T_g.

This study is concerned with an investigation of the effect of changes in the chemical structure of steric stabiliser, nonyl-phenol ethoxylate [NP*X*], (where *X* designates the average chain length of the ethoxylate chain) on the film forming properties of 2-ethylhexylacrylate/methyl methacrylate copolymers latexes (Scheme 1, structure of steric stabiliser).

The location and mobility of the chain in the surface of the latex is determined by the solubility of the ethoxy chain in the aqueous phase. On evaporation of water, the latex particles will come into close contact with other particles and interaction between the steric stabilisation surface layers will occur. Interaction of the ethoxylate chains associated with adjacent particles will generate a region of solvated poly(ethylene glycol) (PEG) chains, which can form either a disordered or partially crystalline phase or disperse in the acrylic phase depending on their molar mass [13]. The ability of the NP*X* to distribute itself between the aqueous and organic phases depends on solubility of the

* Corresponding author. Tel.: +44-141-548-2260; fax: +44-141-548-4822.

E-mail address: r.a.pethrick@strath.ac.uk (R.A. Pethrick).

0032-3861/02/$ - see front matter
PII: S0032-3861(01)00724-8

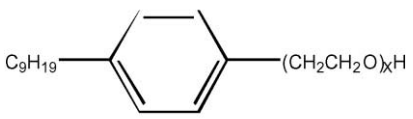

Synperonic NPX, x = 20, 30, 40

Scheme 1.

ethoxy chain length. The crystalline melting point of the PEG tail depends on molar mass and are respectively for NP20—[M_n—880] melting point 305 K; NP30—[M_n—1320] melting point 317 K and NP40—[M_n—1760] melting point 322 K. Crystallisation would increase segregation, inhibit mobility and suppress the possibility of plasticisation of the polymer phase. In this study the latex formulation was kept constant and the only variable was the nature of the steric stabiliser used in the emulsion polymerisation.

2. Experimental

2.1. Materials—latex preparation

Three methyl methacrylate (MMA)/2-ethylhexyl acrylate (EHA) copolymers were prepared, using the method described previously [1]. The total monomer content was ~50 wt% and monomer feed was 34.08 g MMA and 15.9 g EHA. The aqueous phase was buffered with sodium bicarbonate and the polymerisation initiated with potassium persulphate and a second seed of sodium metabisulphite was added half way through the polymerisation. The latex produced was used without further purification. The emulsion process is similar to that used commercially to produce latex materials [2].

3. Latex characterisation

FTIR spectra were obtained from a thin film produced by placing a drop of the latex solution in chloroform on a sodium chloride disc. The spectra were consistent with the monomer formulations and the absence of a band at 1650 cm^{-1} (C=C bond) indicated a low free monomer content. Elemental analysis was carried on the dry polymer and compared with the theoretical values {#}:—coME-NP20—carbon 62.9% {63.3%}, hydrogen 7.7% {6.6%}, oxygen 29.3% {31.1%}; coME-NP30—carbon 57.5% {57.3%}, hydrogen 8.6% {7.0%}, oxygen 33.8% {35.6%} and coME-NP40—carbon 62.7% {62.2%}, hydrogen 7.7% {6.5%}, oxygen 29.5% {31.3%}. The theoretical values were based on the standard formulation summarised in Appendix A. These data are consistent with the above formulations, slight differences can be attributed to retention of water in the latex.

3.1. General latex film characterisation

The latex films were characterised using the following techniques.

Minimum Film Formation Temperature (MFFT). A stainless steel bar heated at one end was used to produce a defined temperature gradient. A latex film of constant thickness was deposited on the heated surface and the temperature at which clear film forms defined the MFFT. The MFFT was measured using thermocouples located along the length of the bar [14].

Glass Transition Temperature (T_g). Differential scanning calorimetry (DSC) measurements were performed using a Perkin–Elmer DSC-2 with a temperature scan from 243 to 403 K at 10 K s^{-1}, at a sensitivity range of 5 mcal s^{-1}. The scans obtained were used to determine the T_g from the onset point, the occurrence of crystalline regions and the heat of coalescence of the latex particles.

Solids Content of the emulsions. The initial and final weight after drying at 80 °C overnight were used to determine the percentage of non-volatiles (%nv);

$$\%\mathrm{nv} = \frac{\text{final weight}}{\text{initial weight}} \times 100 \quad (1)$$

The samples were cooled to room temperature before reweighing in order to minimise the error in the measurement.

Particle Size Determination. A Malvern Autosizer 2C, with a range of measurement from 0.003 to 3 μm, was used to determine the mean particle size of the latex.

Molar Mass Determination. Gel permeation chromatography (GPC) was performed by RAPRA Technology Ltd. using *N*,*N*-dimethylformamide (DMF) as solvent. A Plgel 2X mixed bed-B, 30 cm, 10 μm column was used with DMF buffered with ammonium acetate at an elution rate of 1.0 ml min^{-1}. The GPC system was calibrated with poly(methylmethacrylate) (PMMA) and the results are quoted as 'PMMA equivalent' molar masses.

3.2. Physical characterisation of the latex films formation process

The physical techniques for characterisation of the film forming process depend on whether the latex is in a liquid or semi-solid {touch dry} state. For convenience, the discussion of the methods has been divided into sections; those measurements performed on the liquid state and those performed on the touch dry, semi-solid state.

3.2.1. Stage one of film formation process

The transformation of the liquid latex emulsion into a touch dry solid film was followed by: *dynamic mechanical analysis*. An adapted Rheovibron-DDV II C was used to monitor the change with time of the mechanical properties of a substrate coated with the latex. A No. 1 Whatmann filter paper, 9×45 mm^2 was used as substrate and held between the two clamps, one connected to a stress transducer, the

other to a strain gauge. A force, P, was applied to a strip of material of length, l, and cross sectional area, A, and the stretched length was Δl. The longitudinal stress was P/A and the longitudinal strain $\Delta l/l$. The Young's Modulus of the solid, E, was defined as:

$$\frac{\text{Stress}}{\text{Strain}} = \frac{(P/A)}{(\Delta l/l)} = \frac{Pl}{A\Delta l} = E \tag{2}$$

The strain transducer output was fed to the analogue/digital input of a computer. The stress applied by the rheovibron was fixed and the measured strain depends on the modulus of the sample. A 50 μl of emulsion was applied to the substrate using a micropipette and analysis of the strain was continued until a constant voltage was obtained from the transducer. The output is indicative of the modulus of the substrate. Because the samples of the paper substrate have a variable modulus, the traces are quoted in terms of the voltage variation with time rather than attempting to calculate the absolute modulus. Profiles were obtained at different drying temperatures and the drying rate obtained from the slope of the voltage against time. The slope was obtained by least squares fitting of the data over the linear portion of the curve and allowed calculation of the rate of drying. The rate data were then used to generate an Arrhenius plot:

$$\ln(\text{rate}) = \frac{-E_a}{R}\frac{1}{T} + C \tag{3}$$

where E_a is the activation energy for the film formation process.

3.2.2. Stages two and three of film formation—the maturation of latex films

When the latex film is touch dry, techniques appropriate for examination of solids can be applied to characterise the maturation of the films.

Calorimetric Compensation Method [15–21]. DSC was used to discriminate between reversible and irreversible processes occurring in a latex film. The samples were cast into a flat petri dish and dried for 24 h. Two samples with identical weight (±2%) were placed in sample pans of identical weight (±0.1 mg). The analysis were performed in three consecutive steps:

- *Step* 1—A temperature scan was performed on a dried latex sample against an empty reference pan and the scan was terminated below the latex decomposition temperature.
- *Step* 2—The calorimeter was then cooled to ambient temperature and the sample transferred to the reference holder. A fresh sample was placed in the sample holder and the thermal scan repeated. The sample in the reference holder will display the reversible thermal changes, whereas the fresh sample in the sample holder will show both reversible and irreversible changes. Two types of irreversible change can occur; disappearance of the specific surface of the latex (coalescence) and destruction of crystalline regions in the film. The methylmethacrylate-2-ethylhexyl acrylate copolymer is amorphous, however, regions of crystallinity can arise as a consequence of interactions between extended poly(ethyleneoxide) segments in the long chain surfactant.
- *Step* 3—After cooling a second run was performed to generate a base line.

This method allows identification and separation of reversible and irreversible thermal changes. The method can be applied to the measurement of the enthalpy of coalescence of latex films, the T_g and identification of crystalline domains. The data presented were obtained with 20–30 mg of sample and measured over a temperature range of 243–403 K at a heating rate of 10 K min^{-1} and using a sensitivity range of 10 mcal. The first run exhibits a clear thermal step indicative of the T_g. The second run contains an exothermic peak associated with the coalescence process. The energy of coalescence will be influenced by a number of factors, which include the loss of residual moisture, rearrangement and redistribution of the stabilised layer and the energy associated with the motion of polymer chains moving across the latex interface to form a coalesced film.

The film forming properties will determine the enthalpy of disappearance of the interface between particles. The enthalpy of coalescence will be expected to depend on T_g and the MFFT through their influence on the compaction and deformation of the latex particles. The DSC was standardised using indium, enthalpy of fusion of indium giving a standard deviation of the data obtained as 0.29%.

Atomic Force Microscopy (AFM). A Burleigh AFM [22] was used to investigate the change of the surface structure with ageing time. Latex samples were cast on to a silicon wafer, allowed to dry and scanned at regular intervals in time. Statistical analysis of the image data allowed various roughness parameters to be determined. These are:

Rq—the root mean square of the line/surface, given by:

$$\sqrt{\frac{1}{N}\sum_{i}^{N}(Z_i - Z_{\text{avg}})^2}$$

Ra—the height variance of the line/surface, given by:

$$\frac{1}{N}\sum_{i}^{N}|Z_i - Z_{\text{avg}}|$$

and Rp − p—the height difference between the highest and lowest points on the line/surface, given by: $Z_{\max} - Z_{\min}$.

4. Results and discussion

4.1. General characteristics of the latex polymers

The synthetic procedures used for the preparation of the latex polymers are similar to those used in industry for

Table 1
Characteristics of the polymer latexes

Latex-code	% Non-volatiles	MFF T (K)	Mean particle size (nm)	T_g (K)—DSC	M_w	M_n
CoME-NP20	39.4	314	221	300	938,000	199,000
CoME-NP30	37.7	316	214	308	1,130,000	230,000
CoME-NP40	39.4	319	219	313	995,000	221,000

emulsion paints [2]. The characteristics of the three systems investigated are summarised in Table 1. The percentage of non-volatiles in the final preparation was approximately 50%, which is typical of the latex systems used commercially. No attempt has been made to purify the latex materials, the residual ion content for all the systems studied should be approximately identical. The MFFT and T_{gg} values, measured as indicated above, show an upward drift with increasing chain length, despite the fact that the monomer composition is the same for all the latex materials prepared. The observed changes in the T_g may be inferred as being a consequence of the changes in nature of the stabiliser on the emulsion particles formed. The hydrophobic chains of the surfactant are dispersed in the acrylic phase and for all three stabilisers are all of the same length. The sole difference in the stabilisers is in the length of the ethoxy chain. The observed differences must be attributed to the influence of the stabiliser interactions in the emulsion particles surface layer on the dynamic properties and packing of the polymer in the film formed. The addition of low molar mass additives to a polymeric phase can lead to either a suppression or elevation of the T_g depending upon the relative magnitude of politicisation and antiplasticisation effects. Since the acrylic copolymers all have similar molar masses the effects observed must result from either differences in solubility in the polymer of the stabiliser or differences in the interactions in the surface layer constraining the polymer chains. An increase in the measured value of T_g would imply that NP30 and NP40 were acting as antiplasticisers. However, there is little reason to expect that NP30 and NP40 should have a greater solubility in the acrylic phase than NP20. The measured mean particle size, values of M_w and M_n are all sufficiently close, when one allows for the width distribution in these parameters, for the observed increase in T_g to be attributed, in part, to the effects of constraints in the surface layer imposed by the stabiliser–stabiliser interaction.

4.2. Investigation of the film formation process

4.2.1. Mechanical analysis of film formation

The three latex samples and a paper substrate saturated with water were investigated using a Rheovibron and typical plots of the data obtained are presented in Fig. 1. The (voltage) modulus—time profiles exhibit an initial drop associated with the wetting of the substrate by the latex solution. Two distinctly different drying profiles are

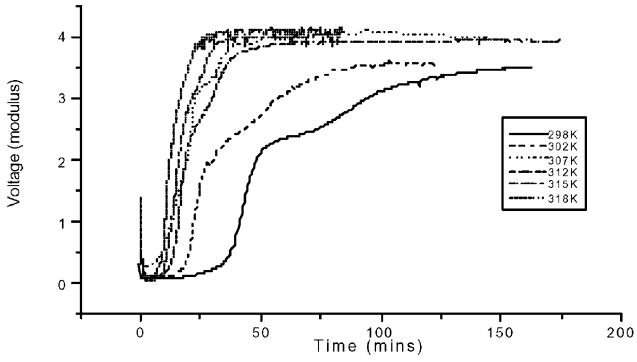

[A]

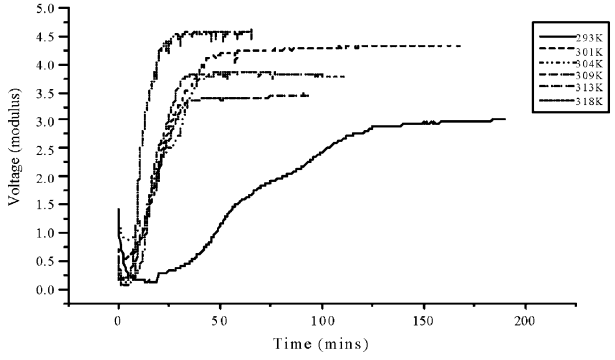

[B]

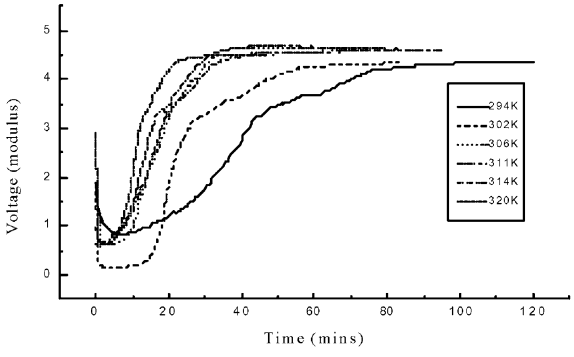

[C]

Fig. 1. Mechanical profile for (A) coME-NP20; (B) coME-NP30 and (C) coME-NP40 drying from filter paper over a range of temperatures.

observed depending on the temperature at which the experiments are conducted. At low temperatures the profile appears to exhibit two stages. An initial fast increase in modulus is followed by a slower process. At high temperatures, the increase in modulus occurs as a single process. In both cases, the final values of the modulus obtained in the long time limit are very similar. The low temperature process exhibits a change in behaviour at a point at which the volume fraction of the emulsion is ~0.7, coinciding with the particles reaching their volume filling limit. At this point, a film will be formed and subsequent increases in the modulus reflect the particles undergoing distortion to form a coalesced film. Below the MFFT, the particle distortions are inhibited and a slower rate of build-up of the modulus is observed. At higher temperatures, the modulus profile exhibits a simple single process in which the modulus increase takes place without interruption at a volume fraction of 0.7. The change in behaviour may be interpreted as being a reflection of the effects of constraints of particle distortion on the film forming process. The MFFT values determined by analysis of the transition from a two stage to a single stage process are close to those obtained by conventional methods, Table 1. The values obtained were coME-NP20—315 K; coME-NP30—313–318 K and coME-NP40—320 K.

The drying rates were obtained from a least squares analysis of the linear portions of the (voltage) modulus—time profiles for each measured temperature, Fig. 1 and Arrhenius plots were constructed, Fig. 2. The values of the activation energies obtained were: 40.3 ± 2.4 kJ mol^{-1} for water, 38.5 ± 7.3 kJ mol^{-1} for coME-NP20, 46.9 ± 8.7 kJ mol^{-1} for coME-NP30 and 37.8 ± 2.8 kJ mol^{-1} for coME-NP40. The similarity between the activation energies for water and latexes indicate that in the first stage the process is predominantly evaporation of water. The second stage of the drying has a higher activation energy E_a which decreased from $X = 20$ to $X = 40$ reflecting a lower degree of hydration due to crystallite formation. The second stage of the drying process below the MFFT is associated with the slow development of interaction between the particles and influenced by the nature of the surface surfactant layer.

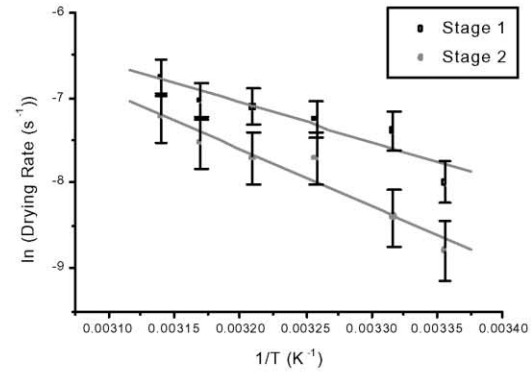

[A]

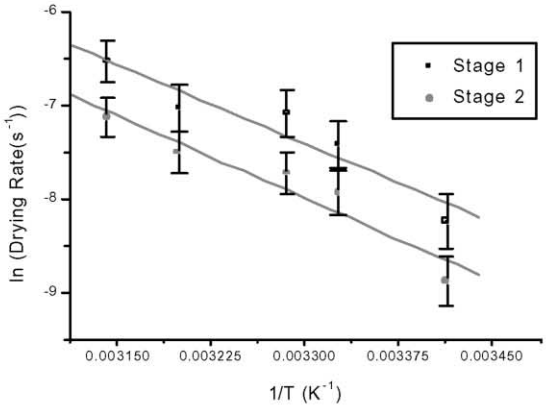

[B]

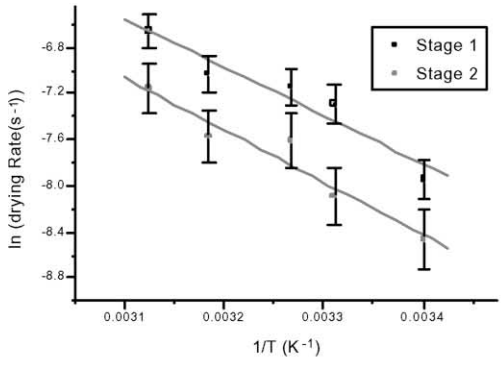

[C]

Fig. 2. Arrhenius plot for the drying of (A) coME-NP20; (B) coME-NP30 and (C) coME-NP40.

4.2.2. Differential scanning calorimetry

DSC measurements were used to characterise the thermal properties of the films. For a typical latex film DSC measurement would be used to measure the T_g, however in this case the measurements can also be used to determine whether or not crystalline phases are present associated with short PEG chains of the interacting surfactant molecules. Using the procedure described above it is also possible to determine the energy of coalescence of the films [24]. DSC thermograms for the pure surfactants, [NP20, NP30 and NP40], used in the emulsion polymerisation were measured and their crystalline melting points determined to be respectively; 305, 331 and 330 K. It is of interest to note that the crystalline melt temperature of NP20 is between the measured T_g and the MFFT. The DSC traces for the NP20 stabilised latex show no evidence for a crystalline melting point either in the films as formed or after 35 days of ageing. In contrast, the films for both the NP30 and NP40 exhibit crystalline melting features once the films are formed, the

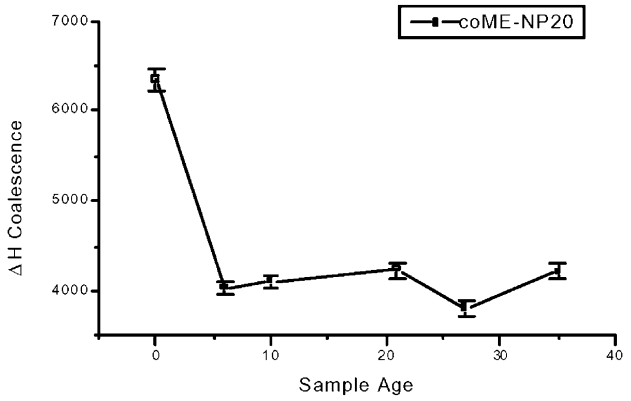

Fig. 3. Variation in the enthalpy of coalescence for coME-NP20.

magnitude and shape of the peak changing with ageing time. For both NP30 and NP40 the melting point of the crystalline phase is above the measured MFFT, Table 1. These films showed evidence of a crystalline melt transition on the high temperature side of the T_g peak. Deconvolution of the crystalline melt and T_g processes proved to be difficult, making it impossible to assess accurately the enthalpy of coalescence for coME-NP30 and coME-NP40. In coME-NP20, the crystallisation peak is absent and the exotherm can be integrated directly.

Integration of the exotherm associated with coalescence for coME-NP20 allowed the degree of coalescence to be quantified, a plot of the variation in the enthalpy of coalescence with sample age measured in days, Fig. 3. The enthalpy of coalescence is high initially and falls sharply in the initial stages of ageing. The observed drop in the enthalpy indicates less energy is required to achieve film formation and implies that over the initial period changes have occurred in the interface, which facilitate film formation. In the later stages of maturation, the enthalpy of coalescence remains relatively static indicating that there is little further change in the extent of surface interaction without an additional input of energy to assist compaction or deformation of the particles.

Comparison of the location of the peaks observed in the DSC traces for the pure surfactants and those for the coMe-NP30 and coMe-NP40 indicate that there is a general correspondence between the transitions in the pure phase and in the latex films [24]. In coME-NP30, the peaks are between 328 and 331 K, the corresponding peak in the surfactant being at 331 K. The observed correspondence implies that the interactions responsible for the formation of crystalline phases in the pure material are also possible in these latex films. The observation of the crystalline melt peak implies that crystalline domains have been created in the region between the polymer particles. The crystalline region in coME-NP40 was observed between 332 and 334 K. The DSC data indicate that whereas in coME-NP40 and coME-NP30 coalescence can be inhibited by crystalline phase formation, in the case of coME-NP20 no such inhibition is occurring.

4.2.3. Atomic force microscopy

Using a micropipette, samples of each of the latexes were cast on to a section of silicon wafer and allowed to dry, and AFM measurements performed. Subsequent scans were taken at various stages of the maturation process, Figs. 4 and 6. The images were then analysed using the AFM statistical analysis software to estimate the changes in surface roughness of the films as they mature. The initial image for each sample displayed in Figs. 4–6, shows the expected close packed pattern for spherical latex particles. Fig. 4 shows that for coME-NP20 close packing is observed and a small amount of deformation occur as the films mature as indicted in image (e). The 32 day images for coME-NP30 and coME-NP40 are also less pronounced than in the earlier scans, however the degree of deformation occurring appear to be much less than in the case of coME-NP20. The scans of coME-NP30 and coME-NP40 also show the presence of voids in the film, an indication that deformation is being inhibited.

The statistical analysis data for the surface roughness, Fig. 7, obtained for the three latex samples over the ageing period studied reveal a decline in the value of the surface roughness as the samples age. The loss of roughness is consistent with the assumption that particles are slowly developing a greater degree of interaction as the films are allowed to mature. In well coalesced emulsion films, it is observed that all traces of the particle surface are lost. In the systems investigated here even after 35 days the shape of the original emulsion particles are easily determined. In contrast, a similar study of related acrylic films using an ionic surfactant demonstrated the changes expected; the initial close packed particles fusing to form a continuous film structure [1,23].

5. Conclusions

The latexes under investigation are identical in monomer composition, only the surfactant is different. The mechanical analysis of the three polymers revealed a two stage drying profile, and conforms to model two of drying. This model defines a point x (the end of stage one) as the point at which the evaporation kinetics are influenced by particle close packing. The subsequent evaporation kinetics are influenced by particle deformation. The form of the drying curve observed are influenced by the mechanism of drying and changes once the MFFT has been exceeded. The activation energies and rate constants calculated for the stage one of the drying processes indicate that it is essentially an evaporation process. Stage two is influenced by two factors; particle deformation and the formation of crystalline domains in the surfactant rich inter particle phase. Such domains would aid the development of the mechanical

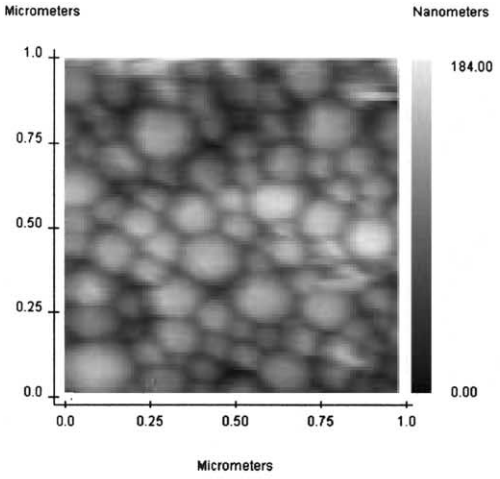

a) - zero

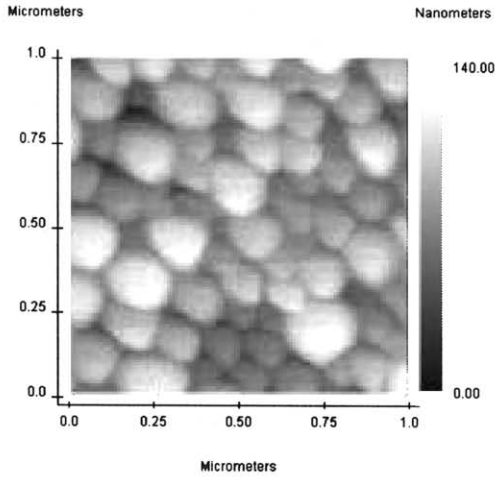

b) - 4 days

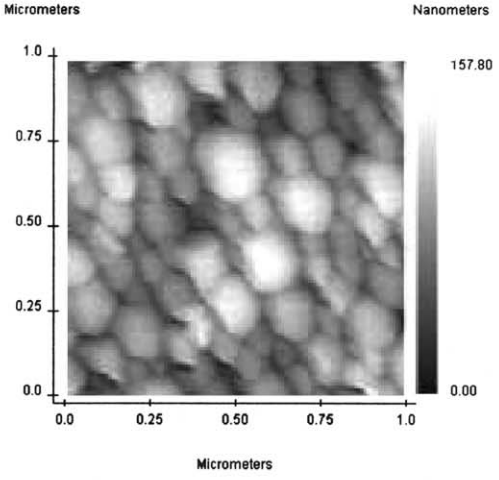

c) - 11 days

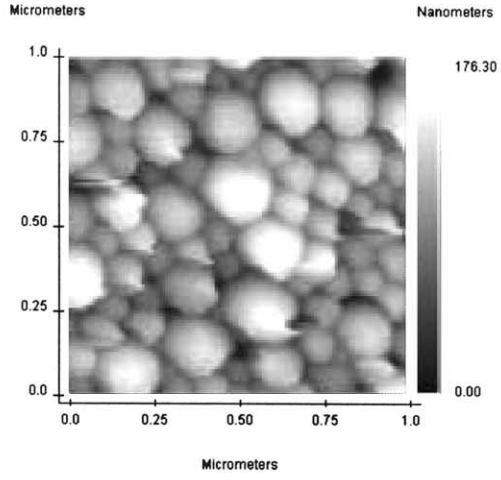

d) - 19 days

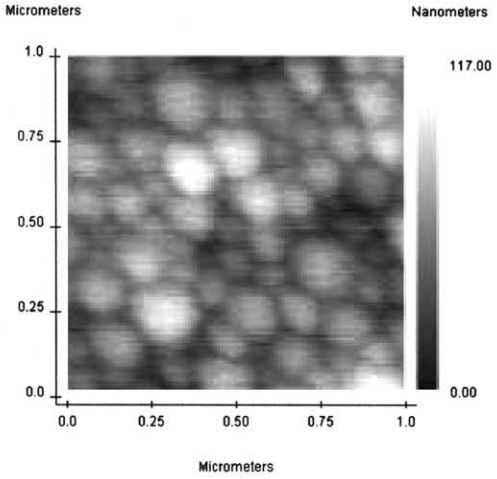

e) - 32 days

Fig. 4. AFM scans of coME-NP20 over a 32 days ageing period.

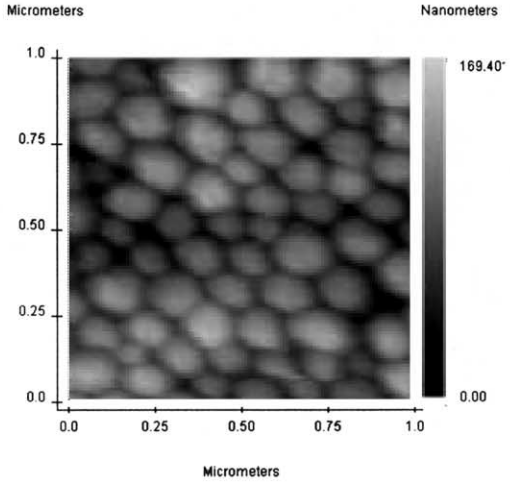

a) - zero

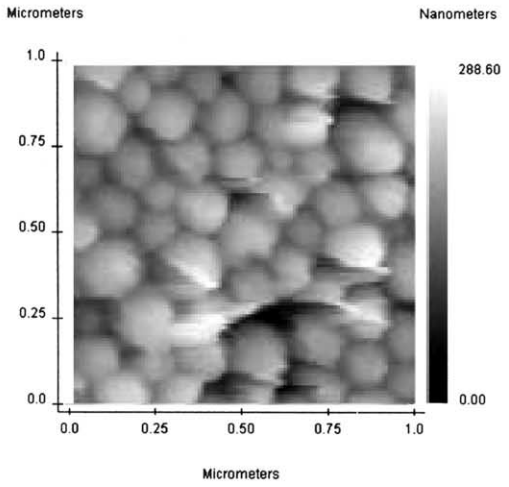

b) - 4 days

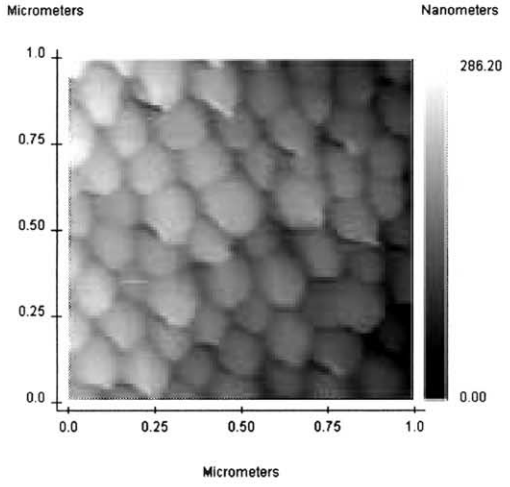

c) - 11 days

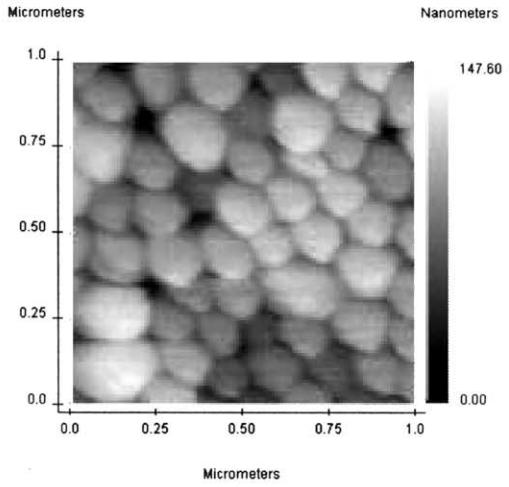

d) - 19 days

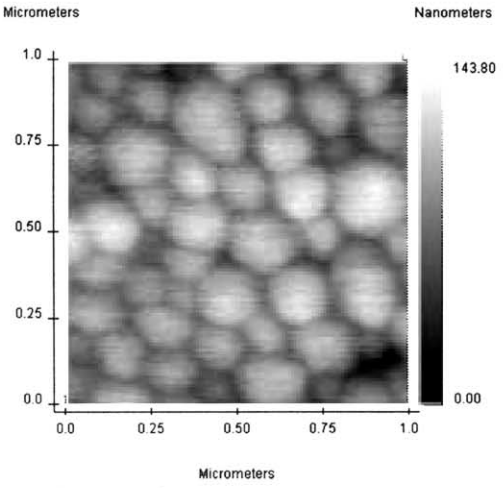

e) - 32 days

Fig. 5. AFM scans of coME-NP30 over a 32 days ageing period.

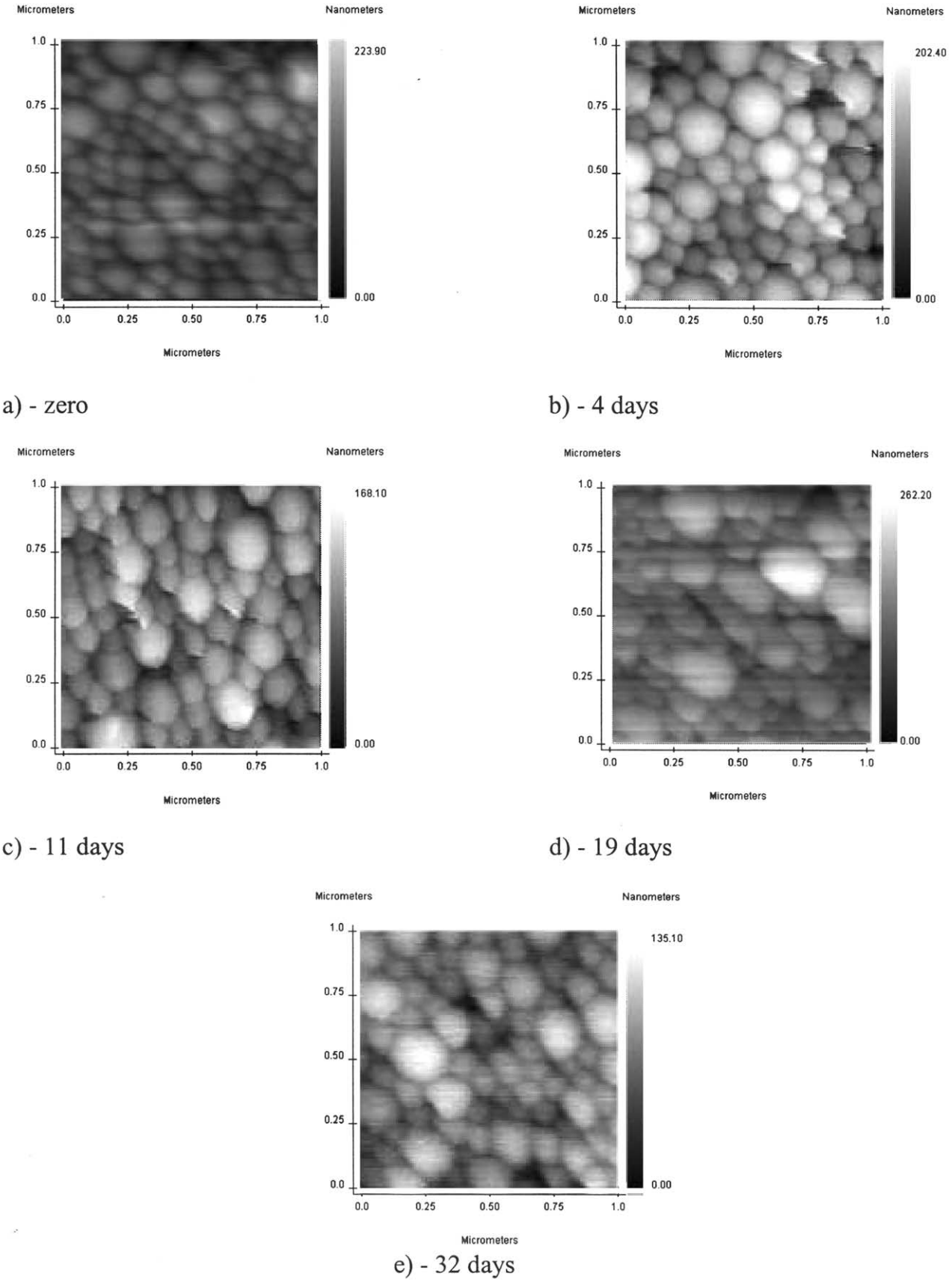

Fig. 6. AFM scans of coME-NP40 over a 32 days ageing period.

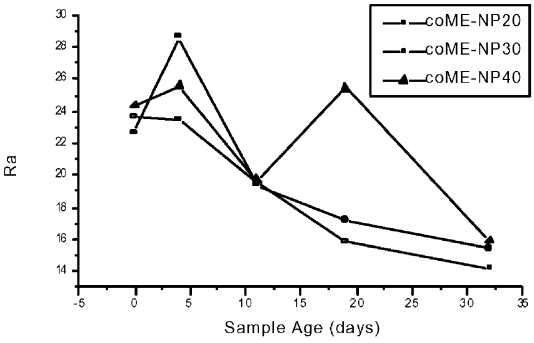

[A]

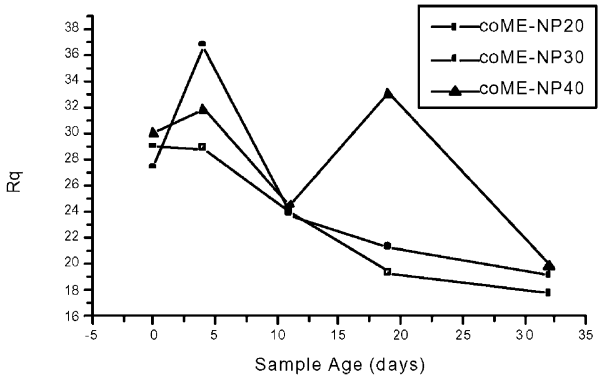

[B]

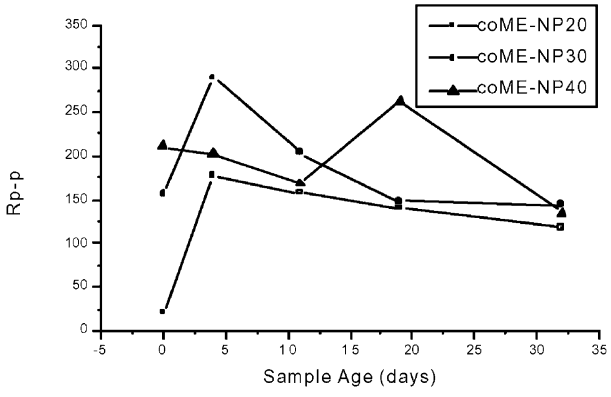

[C]

Fig. 7. (A) Height variance statistical analysis for coME-NPX images; (B) Root mean square statistical analysis of coME-NPX images; (C) Height difference statistical analysis of coME-NPX images.

integrity of the films, but the level of hydration of the inter particulate domain was found to be also influenced.

DSC data confirm the influence of the ethoxylate chain length on the ability to form crystalline domains. These domains made it impossible to determine the enthalpy of coalescence in the materials containing the longer chains lengths. The progress of the film formation process was clearly illustrated by the AFM data, which support the analysis of the model used for interpretation of the other measurements.

Acknowledgements

The support of LAC by EPSRC and ICI in the form of a CASE award is gratefully acknowledged. The interest of Dr David Elliott and Dr David Taylor in the project is also gratefully acknowledged.

Appendix A. Standard formulation used in preparation of latex

The formulation was based on 3.42 g of Synperonic NP*X*, 0.23 g disodium hydrogen phosphate, 0.10526 g potassium persulphate, 0.045 g sodium metabisulphate, 34.08 g methylmethacrylate (MMA), 15.9 g 2-ethylhexylacrylate. Details of the addition procedure and purification methods used are outlined elsewhere [24]. The theoretical values quoted above reflect the actual values of the monomers and surfactants used.

References

[1] Cannon LA, Pethrick RA. Macromolecules 1999;32:7617.
[2] Eckersley ST, Rudin A. Film formation in waterbourne coatings. In: Provder T, Winnik MA, Urban MW, editors. ACS Symposium Series, vol. 648. 1996. p. 2.
[3] Niu BJ, Martin LR, Tebelius LK, Urban MW. Film formation in waterbourne coatings. In: Provder T, Winnik MA, Urban MW, editors. ACS Symposium Series, vol. 648. 1996. p. 301.
[4] Keddie JL, Meredith P, Jones RA, Donald AM. Film formation in waterbourne coatings. In: Provder T, Winnik MA, Urban MW, editors. ACS Symposium Series, vol. 648. 1996. p. 332.
[5] Eu M-D, Ullman R. Film formation in waterbourne coatings. In: Provder T, Winnik MA, Urban MW, editors. ACS Symposium Series, vol. 648. 1996. p. 79.
[6] Winnik MA. Film formation in waterbourne coatings. In: Provder T, Winnik MA, Urban MW, editors. ACS Symposium Series, vol. 648. 1996. p. 51.
[7] Routgh AF, Russel WB. AICHE J 1998;44(9):2088.
[8] Feng JR, Winnik MA. Macromolecules 1997;30(15):4324.
[9] Wang YC, Winnik MA. J Phys Chem 1993;97(11):2507.
[10] Winnik MA, Winnik FM. Advances in chemistry series 236. Washington, DC: American Chemical Society, 1993. p. 485.
[11] Keddie JL, Meredith P, Jones RAL, Donald AM. Macromolecules 1995;28:2673–82.
[12] Sperry PR, Snyder BS, O'Dowd ML, Lesko PM. Langmuir 1994;10:2619.
[13] Keintz E, Holl Y. Colloid Surf A — Physicochemical Engng Aspects 1993;78:255–70.
[14] Mahr TG. J Phys Chem 1970;4:2160.
[15] O'Callaghan KJ, Pain AJ, Rudin A. J Polym Sci Part A, Polym Chem 1995;33(11):1849–57.

[16] Rodriguez F. Principles of polymer systems. 2nd ed. New York: Wiley, 1992.
[17] Harkins WD. J Chem Phys 1945;13:381.
[18] Harkins WD. J Chem Phys 1946;14:47.
[19] Harkins WD. J Am Chem Soc 1947;69:1428.
[20] Harkins WD. J Polym Sci 1950;5:217.
[21] Hayward D, Mahoubian Jones G, Pethrick RA. J Phys E Sci Instrum 1984;17:683.
[22] AFM Reference Manual, Burleigh, 1995.
[23] Cannon L, Hayward D, Pethrick RA. Submitted for publication.
[24] Cannon L. PhD Thesis University of Strathclyde, 1998.